

# Scattering Transform of Heart Rate Variability for the Prediction of Ischemic Stroke in Patients with Atrial Fibrillation

Roberto Leonarduzzi<sup>1</sup>, Patrice Abry<sup>1</sup>, Herwig Wendt<sup>2</sup>, Ken Kiyono<sup>3</sup>,  
Yoshiharu Yamamoto<sup>4</sup>, Eiichi Watanabe<sup>5</sup>, Junichiro Hayano<sup>6</sup>

<sup>1</sup>Univ Lyon, Ens de Lyon, Univ Claude Bernard, CNRS, Laboratoire de Physique, F-69342 Lyon, France;

<sup>2</sup>IRIT, CNRS UMR 5505, University of Toulouse, France;

<sup>3</sup>Division of Bioengineering, Graduate School of Engineering Science, Osaka University, Toyonaka, Japan;

<sup>4</sup>Educational Physiology Laboratory, Graduate School of Education, University of Tokyo, Tokyo, Japan;

<sup>5</sup>Dept of Cardiology, Fujita Health University School of Medicine, Toyoake, Japan;

<sup>6</sup>Dept of Medical Education, Nagoya City University Graduate School of Medical Sciences, Nagoya, Japan;

15 December, 2017

## 1 Summary

**Background.** Atrial fibrillation (AF) is an identified risk factor for ischemic strokes (IS). AF causes a loss in atrial contractile function that favors the formation of thrombi, and thus increases the risk of stroke. Also, AF produces highly irregular and complex temporal dynamics in ventricular response RR intervals. Thus, it is hypothesized that the analysis of RR dynamics could provide predictors for IS. However, these complex and nonlinear dynamics call for the use of advanced multiscale nonlinear signal processing tools.

**Objectives.** The global aim is to investigate the performance of a recently-proposed multiscale and nonlinear signal processing tool, the scattering transform, in predicting IS for patients suffering from AF.

**Methods.** The heart rate of a cohort of 173 patients from Fujita Health University Hospital in Japan was analyzed with the scattering transform. First, p-values of Wilcoxon rank sum tests were used to identify scattering coefficients achieving significant (univariate) discrimination between patients with and without IS. Second, a multivariate procedure for feature selection and classification, the Sparse Support Vector Machine (S-SVM), was applied to predict IS.

**Results.** Groups of scattering coefficients, located at several time-scales, were identified as significantly higher (p-value < 0.05) in patients who developed IS than in those who did not. Though the overall predictive power of these indices remained moderate (around 60%), it was found to be much higher when analysis was restricted to patients not taking antithrombotic treatment (around 80%). Further, S-SVM showed that multivariate classification improves IS prediction, and

also indicated that coefficients involved in classification differ for patients with and without antithrombotic treatment.

**Conclusions.** Scattering coefficients were found to play a significant role in predicting IS, notably for patients not receiving antithrombotic treatment. S-SVM improves IS detection performance and also provides insight on which features are important. Notably, it shows that AF patients not taking antithrombotic treatment are characterized by a slow modulation of RR dynamics in the ULF range and a faster modulation in the HF range. These modulations are significantly decreased in patients with IS, and hence have a good discriminant ability.

**Keywords.** Atrial fibrillation, ischemic stroke, heart rate variability, nonlinear multiscale analysis, scattering transform, wavelet transform.

## 2 Introduction

**Atrial fibrillation.** AF is a supraventricular tachyarrhythmia with uncoordinated atrial activation [1]: The sinus node loses its ability to govern ventricular response [2] and the atrium is depolarized by a chaotic pattern of rapid and random impulses, with two main consequences. First, the atrial tissue contracts in an erratic way, causing the atrial wall to quiver rather than contract [1]. Second, random and high-frequency impulses reaching the AV node cause highly disorganized concealed conduction which results in irregular penetrating impulses [3]. The irregular ventricular response intervals thus generated resemble white-noise fluctuations in the high and low frequency bands (2.5s to 25s), but with more complex dynamics in the very-

and ultra-low bands (from 25s to above 300 s), reflecting circadian rhythms and AV node properties mediated by the autonomous nervous system [1, 2].

**Ischemic stroke.** The impaired mechanical function of the atrium decreases blood flow rates within, and favors thrombi formation and embolic events [1]. Thus, AF is identified as an important risk factor for ischemic strokes (IS) [4], and treatment of AF patients with oral anticoagulants is a mainstay of clinical practice [4]. In consequence, a robust risk stratification scheme of stroke likelihood in AF patients would be of great clinical value, aiding in prophylactic decisions to reduce the exposure of low-risk patients to bleeding complications.

**Related work.** A standard metric to guide antithrombotic therapy in AF patients has been the CHA<sub>2</sub>DS<sub>2</sub>-VASc score, which adds scores obtained from several different risk factors [5]. Also, irregularity measurements from RR dynamics have been proposed, since they share a common origin with atrial mechanisms that favor thrombogenesis and, more importantly, are easy to acquire. However, the complex dynamics of RR series during AF have precluded the application of standard tools —with the notable exception of [6] where time-domain statistical measures were shown to be associated with an increased risk of mortality. More recently, with the advent of finer statistical tools for the analysis of time series, an explicit connection between irregular RR dynamics and IS was explored, e.g. by using multiscale entropy in [7].

### 3 Objectives

Our goal is to investigate the potential benefits of using the scattering transform to characterize the dynamics of RR intervals in AF patients and predict ischemic strokes. This recently-introduced tool, which performs a nonlinear multiscale analysis and provides an informative characterization of time series with complex multiscale dynamics [8, 9], has been successfully used, e.g., for audio classification [9] and acidosis detection in intrapartum fetal heart rate [10].

## 4 Methods

### 4.1 Scattering Transform

**Scattering transform.** Let  $X(t)$  denote the signal to analyze. Let  $\psi(t)$  denote a complex analytic mother wavelet, that is, a band-pass filter supported over positive frequencies. Let  $\psi_j(t) = \{2^{-j}\psi(2^{-j}t), j \in \mathbb{N}\}$  denote the collection of templates of  $\psi$  dilated at scales  $2^j$ . The first-order (or linear) scattering coefficients  $S_1(j_1)$  are defined as the average amplitude of the modulus of

wavelet coefficients  $X \star \psi_{j_1}(t)$ :

$$S_1(j_1) = 2^{-j_1} \sum_{k=1}^{2^{j_1}} |X \star \psi_{j_1}(2^{j_1}k)|, \quad 1 \leq j_1 \leq J. \quad (1)$$

The second-order (or nonlinear) scattering coefficients are defined as the average amplitude of the modulus of a second level of wavelet coefficients:

$$S_2(j_1, j_2) = \frac{2^{-j_2}}{S_1(j_1)} \sum_{k=0}^{2^{j_2}} ||X \star \psi_{j_1} \star \psi_{j_2}(2^{j_2}k)|, j_1 \leq j_2 \leq J. \quad (2)$$

Higher-order scattering coefficients could be defined, accordingly, by further cascading wavelet and modulus operations. We will use only scattering coefficients of first and second orders, as they carry most of the energy in  $X$  [8, 10].

First-order coefficients  $S_1(j_1)$  convey information related to the second-order statistics (correlation, spectrum) of  $X$ , and hence provide a linear analysis. Second-order coefficients  $S_2(j_1, j_2)$  quantify, as a function of scale  $2^{j_2}$ , the temporal dynamics of the nonlinearly transformed wavelet coefficients at scale  $j_1$ ,  $|X \star \psi_{j_1}(t)|$ . They can hence be read as a nonlinear and multiscale representation of the temporal dynamics of  $X$  [8, 10, 11].

### 4.2 Machine learning

A Sparse Support Vector Machine (S-SVM) produces a linear decision  $d$  from features  $\mathbf{x}$  as  $d = \text{sgn}(\mathbf{w}^T \mathbf{x})$ , by finding optimal weights  $\mathbf{w}$  that perform a good classification and only have few nonzero entries. It optimizes a nondifferentiable yet convex functional that balances sparsity in  $\mathbf{w}$  and classification performance (see [12, 13]):  $\hat{\mathbf{w}} \in \text{argmin}_{\mathbf{w} \in \mathbb{R}^P} \|\mathbf{w}\|_1 + C \sum_n \max(0, 1 - y_n(\mathbf{w}^T \mathbf{x}_n))^2$ . The regularization parameter was tuned by cross-validation and grid search to the value  $C = 2^{-3}$  for all classification tasks.

### 4.3 Database

**Data collection.** We analyzed 24-hour-long Holter records from patients suffering from permanent AF (i.e., of more than one year of duration, with no evidence of sinus rhythm, and with no planned sinus rhythm restoration). We excluded patients with complete AV block, sustained ventricular tachycardia, ventricular ectopy > 5%, cardiac pacemakers, paroxysmal AF, heart valves, with more than 5% of the Holter record corrupted by artifacts or noise, taking rhythm-control drugs, or that had acute coronary syndrome, strokes, hemodynamic instability or undergone surgery in the preceding 6 months. This led to a total of 173 subjects, for each of which the CHA<sub>2</sub>DS<sub>2</sub>-VASc score was recorded as a measure of stroke risk [5]. 22 patients, hereafter the *IS patients*, were diagnosed IS by a neurosurgeon during a follow-up period of  $47 \pm 35$

months, as opposed to the 151 remaining *NoIS patients*. Further, 109 (AT) patients received an antithrombotic treatment, while 64 (NoAT) patients did not.

**Ethical considerations.** The study was approved by the ethics committee of Fujita Health University, and conformed to the principles outlined in the declaration of Helsinki. All patients provided written informed consent at the time of Holter recording.

**Recordings.** The Holter ECGs were recorded with a 2-channel digital recorder (Fukuda Denshi, Tokyo) and digitized at a 125 Hz sampling frequency and 12 bit resolution. RR intervals were detected automatically, with manual review and editing by experts.

**Preprocessing.** First, outliers were removed: RR intervals were excluded according to the following rules: (i) interval smaller than 350 ms, or ii) interval larger than 3500 ms, or iii) interval 2.5 times larger than the local 90% percentile. The resulting time series were visually inspected to verify the absence of outliers. Finally, the filtered RR series was uniformly resampled at 2 Hz using linear interpolation.

## 5 Results and discussion

**Scattering coefficients.** Fig. 1 shows coefficients  $\log_2 S_1$  (left),  $\log_2 S_2(j_1 = 4, j_2)$  (middle), and  $\log_2 S_2(j_1 = 10, j_2)$  (right) for IS (red crosses) and NoIS (blue circles) patients. As expected,  $\log_2 S_1$  reproduces the power spectrum of the data and matches the behavior documented in [2]: Two scaling regimes, for  $j \in [2, 8]$  ( $\approx [2, 120]$  s) and  $j \in [9, 13]$  ( $\approx [4, 70]$  min), with a cutoff scale  $j_c = 8 \approx 2$  min, are in agreement with [2, 7]. However, it can also be seen that  $\log_2 S_1$  is remarkably similar for both classes and thus unsuitable for discrimination.

In contrast,  $\log_2 S_2$  shows significant differences for several pairs of octaves  $(j_1, j_2)$ : Fig. 1 (right) shows that  $\log_2 S_2(j_1 = 10, j_2)$  is clearly able to discriminate between the two classes; and slight differences are seen for  $j_2 \in [5, 8]$  in Fig. 1 (middle). Notably, *IS patients* show lower  $\log_2 S_2$ , indicating that their HR dynamics are characterized by less nonlinear variability.

**Univariate classification performance.** To assess discriminatory power, Wilcoxon ranksum tests were performed independently on  $\log_2 S_1(j_1)$  for each  $j_1$ , and on  $\log_2 S_2(j_1, j_2)$ , for each  $(j_1, j_2)$ . No linear scattering coefficients  $\log_2 S_1(j_1)$  yielded significant differences, while the  $\log_2 S_2(j_1, j_2)$  were found significant for several pairs  $(j_1, j_2)$ .

First, coefficients  $\log_2 S_2(j_1, j_2)$  that were found to be significant were tracked. Second, significant  $\log_2 S_2(j_1, j_2)$  that share the same main scale  $2^{j_1}$  and contiguous secondary scales  $2^{j_2}$  were grouped together as a single feature, since they correspond to temporal dynamics in the same frequency ranges. This resulted in four groups, as indicated in Table 1. Wilcoxon ranksum tests were performed on averaged

$\log_2 S_2(j_1, j_2)$  in each group, yielding significant differences between classes (p-values reported in Table 1), for a wide range of time scales  $2^{j_1}$  (ranging from  $\approx 2$  s to  $\approx 512$  s). Coefficients SG4 quantify a slow modulation (from 17min to 1h) of the HR dynamics in the ultra low frequency (ULF) range (scales larger than 8.5 min), while SG1, SG2 and SG3 indicate an intermediate modulation (from 16 s to 1 or 2 min) of the HR dynamics at the *finest time scales* (from  $\approx 2$  to  $\approx 8$  s, HF range). Notably, no scattering coefficients yield significant differences for primary scale  $2^{j_1}$  in the very low frequency (VLF) range, where multiscale entropy was found to be significant in [7], but the modulation scales  $2^{j_2}$  correspond largely to the VLF region for the first three groups.

S-SVM multivariate classification was applied to features consisting of the 4 groups of scattering coefficients, to which EN and the  $\text{CHA}_2\text{DS}_2\text{-VASc}$  score (CHA) were added for comparison. Fig. 2 displays the *weights* assigned by the S-SVM to each feature. First, it shows that the analysis of *All* subjects leads to a nonsparse decision rule that involves all features. On the contrary, classification is much sparser when analyzing *AT* and *NoAT* patients independently, with very different features selected in each case. For *NoAT* patients, scattering coefficients are predominantly selected, while for *AT* patients, CHA and EN are essentially selected. Scattering coefficients are hence quantifying HR temporal dynamics that have a direct incidence on the formation of thrombi and thus in the outcome. On the contrary, when AT drugs are used, the  $\text{CHA}_2\text{DS}_2\text{-VASc}$  score rises as the main predictor, associated with outcomes that do not depend on atrial thrombosis. Second, while classification performance quantified by the Area under ROC Curve (AUC) remains modest for *All* and *AT* patients ( $\approx 0.65$ ), it is much improved for *NoAT* patients ( $\approx 0.85$ ).

**Univariate versus multivariate classification performance.** Univariate performances for each feature (including EN and CHA) are compared against S-SVM performance in Fig. 3. For all patients, features EN, SG1, SG2, SG3 and SG4 all perform individually better than the standard CHA, and S-SVM classification does not improve performance. When analysis is restricted to *AT* patients, predictive power is poor, and CHA shows the best performance, while nonlinear features EN, SG1, SG2, SG3 and SG4 perform poorly. While S-SVM improves on all nonlinear features, it does not outperform CHA. On the contrary, for *NoAT* patients, performance is high—notably for SG4 reaching almost 80%. S-SVM further increases performance significantly—above 85%—by selecting mostly SG3 and SG4. This shows that the slow modulations of the RR dynamics in the ULF range (SG4), and HF range (SG3), play a significant role in predicting IS for *NoAT* patients.

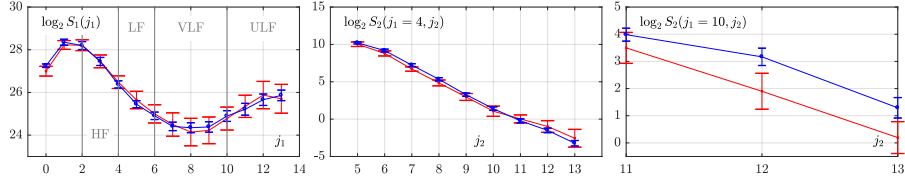


Figure 1: Coefficients  $\log_2 S_1(j_1)$  (left),  $\log_2 S_2(j_1 = 4, j_2)$  (middle), and  $\log_2 S_2(j_1 = 10, j_2)$  (right), as a function of  $\log_2 j$ , for the RR time series of patients that did (red crosses) and did not (blue crosses) develop ischemic strokes (median and 95% confidence intervals).

Table 1: Definition of groups and p-values.

Group	$j_1$	$j_2$	p-value
SG1	2 (2 s, HF)	[5, 7] ([16 s , 1 min ], LF-VLF)	0.039
SG2	3 (4 s, HF)	[5, 8] ([16 s , 2 min ], LF-VLF)	0.048
SG3	4 (8 s, HF)	[5, 8] ([16 s , 2 min ], LF-VLF)	0.005
SG4	10 (8.5 m, ULF)	[11, 13] ([17 min , 1 h ], ULF)	0.022

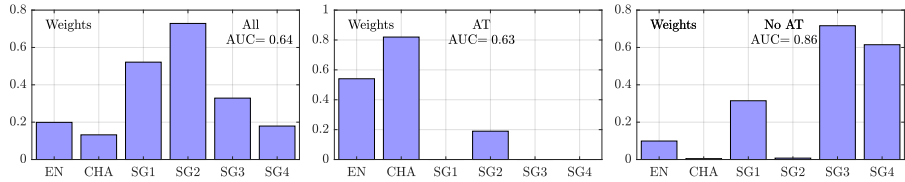


Figure 2: S-SVM classification: Weights  $\mathbf{w}$  for all patients (left), and those with antithrombotic treatment (AT, middle) and without it (NoAT, right). For ease of comparison, AUC obtained by S-SVM is printed onto each plot.

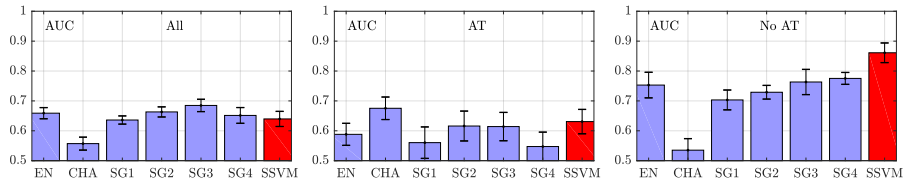


Figure 3: AUC (and 95% confidence intervals computed from 5-fold cross-validation) for each feature individually, and for the S-SVM multivariate classification, for all patients (All), patients with (AT) and without (NoAT) antithrombotic treatment.

## 6 Conclusions

Results obtained here suggest the promising value of features based on the scattering transform, as well as multiscale entropy, as predictors of ischemic stroke—in particular when patients are not undergoing antithrombotic treatment. Results emphasize that relevant information is encoded in nonlinear dynamics not accessible from simpler spectral techniques, and showcase the large discriminatory power provided by a cascade of *simple* operators in the scattering transform. They also show that S-SVM, performing jointly feature selection and classification, achieves improved classification performance. Notably, results show that activity in the HF range—previously considered to be random noise under AF—is discriminant. Further research is needed to understand the physiological mechanisms

for these nonlinear modulations in the HF range.

## Acknowledgements

This work was supported by CNRS grant PICS 7260.

## References

1. Kirchhof P, Benussi S, Kotecha D, Ahlsson A, Atar D, Casadei B. Guidelines for the management of atrial fibrillation developed in collaboration with EACTS. *Eur Heart J.* 2016;273(37):2893–2962.
2. Hayano J, Yamasaki F, Sakata S, Okada A, Mukai S, Fujinami T. Spectral characteristics of ventricular response to atrial fibrillation. *Am J Physiol Heart Circ Physiol.* 1997;273(6):H2811–H2816.

3. Kirsh JA, Sahakian AV, Baerman JM, Swiryn S. Ventricular response to atrial fibrillation: role of atrioventricular conduction pathways. *J Am Coll Cardiol.* 1988;12(5):1265–1272.
4. Fuster V, Rydén LE, Cannom DS, Crijns HJ, Curtis AB, Ellenbogen KA, et al. ACC/AHA/ESC 2006 Guidelines for the Management of Patients With Atrial Fibrillation. *Circulation.* 2006;114(7):e257–e354.
5. Lip GY, Frison L, Halperin JL, Lane DA. Identifying Patients at High Risk for Stroke Despite Anticoagulation. *Stroke.* 2010;41(12):2731–2738.
6. Yamada A, Hayano J, Sakata S, Okada A, Mukai S, Ohte N, et al. Reduced ventricular response irregularity is associated with increased mortality in patients with chronic atrial fibrillation. *Circulation.* 2000;102(3):300–306.
7. Watanabe E, Kiyono K, Hayano J, Yamamoto Y, Inamasu J, Yamamoto M, et al. Multi-scale Entropy of the Heart Rate Variability for the Prediction of an Ischemic Stroke in Patients with Permanent Atrial Fibrillation. *PLOS ONE.* 2015;10(9):e0137144.
8. Mallat S. Group Invariant Scattering. *Comm Pure Appl Math.* 2012;65(10):1331–1398. ArXiv: 1101.2286.
9. Andén J, Mallat S. Deep Scattering Spectrum. *IEEE Trans Sig Proc.* 2014;62(16):4114–4128.
10. Chudáček V, Andén J, Mallat S, Abry P, Doret M. Scattering Transform for Intrapartum Fetal Heart Rate Variability Fractal Analysis: A Case-Control Study. *IEEE Trans Biomed Eng.* 2014;61(4):1100–1108.
11. Bruna J, Mallat S, Bacry E, Muzy J. Intermittent process analysis with scattering moments. *Ann Statist.* 2015 02;43(1):323–351.
12. Blondel M, Seki K, Uehara K. Block coordinate descent algorithm for large-scale sparse multiclass classification. *J Mach Learn.* 2013 Oct;93(1):31–52.
13. Spilka J, Frecon J, Leonarduzzi R, Pustelnik N, Abry P, Doret M. Sparse Support Vector Machine for Intrapartum Fetal Heart Rate Classification. *IEEE Journal of Biomedical and Health Informatics.* 2016;PP:1–1.